HOKKAIDO UNIVERSITY

Title	Blocking of oestrogen signals improves anti-tumour effect regardless of oestrogen receptor alpha expression in cancer cells
Author(s)	Kajihara, Nabeel; Ge, Yunqi; Seino, Ken-ichiro
Citation	British journal of cancer, 129(6), 935-946 https://doi.org/10.1038/s41416-023-02381-0
Issue Date	2023-10-05
Doc URL	https://hdl.handle.net/2115/93015
Rights	This version of the article has been accepted for publication, after peer review (when applicable) and is subject to Springer Nature's AM terms of use, but is not the Version of Record and does not reflect post-acceptance improvements, or any corrections. The Version of Record is available online at: http://dx.doi.org/10.1038/s41416-023-02381-0
Type	journal article
File Information	72134_3_merged_1689730203.pdf, main text

Hokkaido University Collection of Scholarly and Academic Papers : HUSCAP

Blocking of estrogen signals improves anti-tumor effect regardless of estrogen receptor alpha expression in cancer cells

Nabeel Kajihara[1], Yunqi Ge[1], Ken-ichiro Seino[1*]

Author affiliations

[1]Division of Immunobiology, Graduate School of Medicine, Institute for Genetic Medicine, Hokkaido University, Kita-15 Nishi-7, Sapporo 060-0815, Japan

E-mail addresses

Nabeel Kajihara: nabeel@igm.hokudai.ac.jp; Yunqi Ge: Kaunki@igm.hokudai.ac.jp

Corresponding author (*)

Ken-ichiro Seino, M.D., Ph.D.

Division of Immunobiology, Graduate School of Medicine, Institute for Genetic Medicine, Hokkaido University, Kita-15 Nishi-7, Sapporo 060-0815, Japan

Tel: 81-11-706-5532, Fax: 81-11-706-7545, E-mail: seino@igm.hokudai.ac.jp

Abstract

Background: Anti-estrogenic therapy has been used for breast cancer patients with estrogen susceptibility cancer cells. However, little has been known about its potential role for immune cell biology within TME, particularly in cancer patients without estrogen sensitivity of tumor cells. Therefore, we aimed to study the effect of estrogen on immunity within TME.

Methods: Using a clinical dataset, immune cells of humans and mice, female mice with and without ovaries, and several murine ERα-negative cancer cell lines, we evaluated the effect of estrogen on immunity in TME.

Results: Clinical data analysis suggested estrogen's suppressive efficacy against CTLs. Additionally, in vitro and in vivo experiments revealed intra-tumoral CTLs' direct repressive action by estrogen in both mice and humans; blockade of estrogen signals canceled its immunosuppression resulting in tumor growth reduction in vivo. Most notably, immunotherapy (immune checkpoint inhibitor; ICI) combined with anti-estrogenic therapy exhibited a dramatic anti-tumor effect.

Conclusions: This study provides novel insights into how estrogen contributes to tumor progression and a therapeutic rationale for blocking estrogen signaling to boost the anti-tumor effect of ICI, regardless of tumor cells' ERα expression.

Keywords

Estrogen, ER, Estrogen signal, Anti-estrogenic therapy, TME, CTL, ERα-negative cancer, TNBC, ICI

Background

Estrogen is a sex steroid hormone present in all vertebrates and responsible for sexual development, including regulating the female reproductive system and breast [1, 2]. In premenopausal women, estrogen is predominantly produced by the ovary and is negligibly produced after menopause [1]. Besides, estrogen is also used as a medication for menopausal hormone therapy and hormonal birth control [3]. The actions of estrogen are mediated by the estrogen receptor (ER), a nuclear protein that binds to deoxyribonucleic acid (DNA) and regulates various gene expressions [4]. ER has two isoforms, ER alpha (ERα) and ER beta (ERβ); they are expressed not only in specific tissues such as the ovary, uterus, and breast but also in most immune cells [5]. Like other steroid hormones, estrogen passively enters the inside of the cell, then binds to the ER and activates it [4]. Thereby, ER activates signal transduction molecules, such as mitogen-activated protein kinase (MAPK) and phosphoinositide 3-kinase (PI3K), initiating cell survival and proliferation signals [6]. Consequently, the deregulation of ER-mediated signaling has possible cause mammary tumorigenesis and ovarian/endometrial carcinogenesis [7].

The importance of the estrogen-ER axis in cancer initiation and progression is emphasized by previous reports that early menstruation and late menopause, namely long-term exposure to estrogen, are related to a high breast cancer incidence [8]. Notably, about 75% of breast cancer cases are ERα-positive at diagnosis, which means they are sensitive to estrogen

[9]. On the other hand, ERα-positive cases are responsive to anti-estrogenic therapies as endocrine therapies, and hence ERα positively in cancer cells is associated with a better prognosis [10]. Certainly, anti-estrogenic therapies by estrogen synthesis suppression or ER inhibition used to treat ERα-positive breast cancer patients remain one of the most successful targeted therapies in anti-cancer therapy [11]. By contrast, ERα-negative tumors such as triple-negative breast cancer (TNBC), characterized by a lack of therapeutic targets, are more aggressive and metastatic, as evidenced by the report that ERα expression in cancer cells is inversely correlated with lymph node metastasis [12]. Moreover, they are refractory to most anti-cancer therapies, wherein obstacles imposed by the tumor microenvironment (TME) contribute significantly [13].

The TME, which contains various immune system elements, dominates the fate of the tumor [14]. Indeed, noninflamed-TME with low infiltration of immune cells or high infiltration of immunosuppressive immune cells correlates with poor prognosis; meanwhile, inflamed-TME accompanied by many anti-tumor immune cells, such as cytotoxic T lymphocytes (CTLs) infiltration, correlates with better clinical outcomes [15]. Although the role of estrogen in anti-tumor immunity is not well understood, previous studies reported that estrogen accelerates tumor progression by driving the mobilization and immunosuppressive activity of myeloid-derived suppressor cells (MDSCs) or macrophages [16, 17]. Besides, estrogen can modulate lymphocyte cytokine production and effector cells' activation via their ER and indeed directly

suppresses T cell-mediated immune response in vitro [5, 18]. Likewise, in vivo, an increase in estrogen levels during pregnancy reduced activated lymphocytes [19, 20]. Furthermore, it is worth noting that men are more responsive to immune checkpoint inhibitors (ICIs) than women [21]. Based on these backgrounds, it is evident that the estrogen-ER axis participates in orchestrating TME, wherein immune cells are considered the potential target in estrogen-induced immunosuppression.

Since the dynamics of the estrogen-ER axis in immune cells of TME hitherto have been poorly understood, this study focused on the relationship between estrogen and anti-tumor immunity. From the clinical data analysis, we postulated that one mechanism of immunosuppressive TME creation could be through estrogen-mediated suppression of CTLs and explored this by mainly using mouse tumor models. Consequently, ER antagonists lifted estrogen-induced immunosuppression, notably CTLs' repression, in tumor cells' ERα-independent manner resulting in tumor volume reduction. Besides, combination therapy of ICI and ER antagonists led to drastic anti-tumor effects, suggesting that anti-estrogenic therapy has the potential to maximize the therapeutic efficacy of cancer immunotherapy. The present study demonstrates hitherto poorly understood dynamics of estrogen in tumor-cell ERα-independent manner in the TME, providing a new rationale for cancer immunotherapy that most cancer patients have not benefited from it yet.

Results

Estrogen-inducible enzyme HSD17B1 inversely correlates with intra-tumoral CTLs' infiltration and induces poor outcomes in TNBC patients

ERα-negative cancers, including TNBC tumors, have been generally considered unaffected by estrogen. Recently, it was revealed that tumor-infiltrating immune cells express ERα [22], but the effects of estrogen in the TME of ERα-negative tumors have not been fully clarified. To address this issue, we investigated the relationship between estrogen and each immune cell using gene expression datasets of TNBC tumors.

There are three estrogens inside the vertebrate body: estrone (E1), estradiol (E2), and estriol (E3), present at almost equal levels [23]. In particular, E2 has the most potent estrogenic hormonal activity and is produced from testosterone or E1 by enzymes encoded by genes such as CYP19A1 and HSD17B1 [24]. 17β-HSD1 encoded by HSD17B1 catalyzes the last step in estrogen activation by converting androgen to testosterone and E1 to E2 [25]; namely, 17β-HSD1 is essential for producing E2 and comprehensively controls estrogenic activity.

When we analyzed the TNBC patients' datasets registered in The Cancer Genome Atlas (TCGA), although there was no relationship between HSD17B1 and myeloid cell-related genes (Fig. S1), HSD17B1 and effector lymphocyte-related genes, such as PRF1, GZMB, IFNG, CD3E, CD69, and CD8A, were negatively correlated (Fig. 1a). Incidentally, no meaningful correlation existed between CYP19A1 and effector lymphocyte-related genes (Fig. S2). Given

these results, we then examined the association between HSD17B1 and CTL (=$CD8^+$ T cell) subset abundance within tumors using the TIMER2.0 web server, which estimates intra-tumoral immune infiltration levels for TCGA; there was an evident inverse correlation between the two elements (Fig. 1b). Besides, high HSD17B1 expressing TNBC patients had lower intra-tumoral CTL infiltration (Fig. 1c) and showed significantly poor prognosis (Fig. 1d) compared to TNBC patients with low HSD17B1. It should note that TNBC cells express ERβ (gene name: ESR2) and G protein-coupled estrogen receptor 1 (GPER1, gene name: GPER) even though they do not express ERα, and these genes contribute to a good prognosis rather than a poor prognosis [26]. Therefore, we also evaluated the value of ESR2 and GPER in TNBC prognosis. However, in the dataset we analyzed in this study, there was no correlation between ESR2 or GPER and CTL infiltration in the tumor (Fig. S3a, b), nor did their expression affect prognosis (Fig. S3c, d). Although myeloid cells' suppression by estrogen in the TME has been previously reported [17, 22], our results suggest that estrogen suppresses CTLs, resulting in a poor prognosis, even in ERα-negative cancers in an ERβ- and GPER1-independent manner.

Estrogen promotes tumor growth and shortens survival by mediating the immune system of ERα-negative cancers

Based on the analyses of gene expression datasets in human tumors, we hypothesized that estrogen influenced the prognosis of ERα-negative cancers by modulating TME, particularly

CTLs, and tested it using the mouse model. We first checked the expression of ER in mouse TNBC 4T1 and mouse colon cancer CT26 cell lines (Fig. 2a and Fig. S4a) and confirmed that both 4T1 and CT26 cells themselves are unresponsive to estrogen (Fig. 2b). Human ER-positive breast cancer T47D, used as a positive control, showed ERα expression and responsiveness to estrogen (Fig. 2a and Fig. S4b).

To determine whether estrogen affects tumor progression and TME of ERα-negative cancers, we performed ovariectomy against female mice and generated estrogen-depleted models (OVX mice). When we transplanted 4T1 or CT26 cells into OVX or sham-operated mice, OVX mice reduced tumor progression compared to control mice in both tumor models (Fig. 2c). At the time of tumor harvest, we confirmed a marked reduction of OVX mice tumors' weight compared to control tumors (Fig. S5a). In contrast, daily administration of estrogen into OVX mice reversed tumor reduction efficacy caused by OVX and increased uterine weight (Fig. 2c and Fig. S5a, b).

Supporting the above results, estrogen-insensitive tumor-bearing OVX mice prolonged survival compared to untreated control mice; contrary to this, estrogen supplementation to OVX mice invalidated the survival benefit of OVX (Fig. 2d). Most notably, tumor regression efficacy by OVX, which was observed in wild-type mice, disappeared in nude mice (Fig. 2e), indicating that T cell immunity is required for estrogen depletion-derived tumor reduction. These data

collectively demonstrated that estrogen induces tumor progression and poor outcomes by mediating the immune system in ERα-negative cancers.

Anti-estrogenic therapy reduces tumor growth via improving TME in ERα-negative cancers

To further consolidate the view that estrogen promotes tumor growth independently of tumor cell ERα expression, we asked whether anti-estrogenic therapy shows anti-tumor effects against ERα-negative cancers. Of note, fulvestrant, a selective ER down-regulator known as the most effective ER antagonist currently available for clinical use [27], remarkably suppressed ERα-negative cancers' growth in the syngeneic tumor transplanted mouse model (Fig. 3a and Fig. S6a). As a pharmacodynamic analysis, sufficient drug dosage has been confirmed by measuring uterine weight (Fig. S6b). Although there are reports that fulvestrant contributes to tumor suppression by modulating ERβ expression in TNBC cells [28, 29], it is barely expressed in the 4T1 tumors used in this study, and fulvestrant administration did not alter ERβ expression within tumors in our experimental system (Fig. S6c).

To understand how fulvestrant affects the TME, we analyzed the tumor-infiltrating immune cell repertoire using flow cytometry. Within the 4T1 tumors treated with fulvestrant, a decrease in MDSCs and an increase in macrophages and T cells were observed (Fig. 3b). When we analyzed macrophages' fractions in detail, in the fulvestrant-treated group, M1-macrophages: that promote immune responses were increased; meanwhile, M2-macrophages

involved in immunosuppression were decreased (Fig. 3c). In tumor-infiltrating T cells' subsets, fulvestrant drastically increased not $CD4^+$ but $CD8^+$ T cells (Fig. 3d), and besides, it increased interferon-γ^+ cells among $CD8^+$ T cells (Fig. S6d). Notably, fulvestrant induced higher gene expression of granzyme-b, perforin-1, and interferon-γ within the tumors, suggesting that fulvestrant induces and activates effector CTLs (Fig. 3e). On the other hand, within the CT26 tumors treated with fulvestrant, there was no change in the infiltration level of M1-macrophages, M2-macrophages, and MDSCs, and we observed an increase in only intra-tumoral T cells, particularly $CD8^+$ T cells (Fig. S6e, f). Namely, it was revealed that fulvestrant consistently altered the T cells (particularly $CD8^+$ T cells) population in ERα-negative cancers.

To further confirm our findings that blocking estrogen signaling leads to tumor reduction even in ERα-negative tumors, we treated TNBC using anti-estrogenic agents other than fulvestrant, specifically tamoxifen: a selective ER modulator, and anastrozole: an aromatase inhibitor. In the estrogen-ER axis, tamoxifen was used as an inhibitor of the receptor side, same as fulvestrant; by contrast, anastrozole was used as an inhibitor of the ligand side [30]. Consequently, both tamoxifen and anastrozole significantly suppressed TNBC tumor growth with changes in uterine weight (Fig. S7a, b, and d); moreover, they consistently increased $CD8^+$ T cells within the TNBC tumors (Fig. S7c, e). These observations overall suggest that estrogen promotes tumor growth, and its inhibitors can suppress tumor progression by increasing intra-tumoral effector CTLs in ERα-negative cancers.

Anti-estrogenic therapy directly activates and increases intra-tumoral effector CTLs by releasing estrogen-mediated suppression of CTL-derived IL-2 expression

We next asked how anti-estrogenic therapy increases $CD8^+$ T cells in ERα-negative tumors. Before addressing this issue, we first evaluated the importance of $CD8^+$ T cells in tumor reduction by anti-estrogenic therapy. Because anti-CD8 antibody administration canceled fulvestrant-derived tumor reduction in TNBC (Fig. 4a, b), $CD8^+$ T cells dependency in anti-estrogenic therapy against ERα-negative cancers was demonstrated. Then we assessed the relationship between estrogen and $CD8^+$ T cells. Interestingly, estrogen directly suppressed the increment in $CD8^+$ and $CD8^+CD69^+$ T cells both in humans and mice, and fulvestrant restored the estrogen-induced $CD8^+$ T cell suppression (Fig. 4c and Fig. S8). These results show that estrogen directly suppresses the proliferation and activation of CTLs, and anti-estrogenic therapy can altogether cancel its adverseness.

As direct suppression of CTLs by estrogen was revealed, we then assessed its detailed mechanism. It has been known that IL-2 influences T cell differentiation and proliferation, such as CTLs, and is a critical determinant of the fate of not only $CD4^+$ but also $CD8^+$ T cells [31]. Notably, IL-2 produced by $CD8^+$ T cells enables their optimal population expansion through an autocrine pathway [32]. In addition, high levels of IL-2 favor the development of effector $CD8^+$ T cells [33]. Based on these contexts, we hypothesized that estrogen might function as a modulator of IL-2 signals in $CD8^+$ T cells within the TME. Indeed, estrogen exposure to $CD8^+$

T cells dramatically suppressed IL-2 mRNA levels (Fig. 4d), and estrogen concentration-dependently reduced IL-2 protein production (Fig. 4e). By contrast, fulvestrant released suppression of IL-2 production from $CD8^+$ T cells by estrogen (Fig. 4d, e). Most notably, the anti-tumor efficacy of fulvestrant against TNBC was abolished by IL-2 inhibition (Fig. 4f, g). At the time of tumor harvest, we checked tumor-infiltrating $CD8^+$ T cells and confirmed that IL-2 inhibition disappeared proliferation and activation of $CD8^+$ T cells by fulvestrant, and each level lifted by fulvestrant turned back to baseline (Fig. S9).

To identify the critical regulator within CTL that modulates the IL-2 production level, we analyzed each CTL treated with estrogen or estrogen plus fulvestrant by RNA-seq. When we performed gene ontology analysis using gene lists obtained from RNA-seq, it was revealed that estrogen suppressed the JAK-STAT pathway in CTLs, and the fulvestrant released its repression (Fig. 4h). The JAK-STAT pathway is closely related to IL-2-mediated T cell activation and proliferation, with STAT3/5, in particular, serving as master regulators in T cell function [34]. Therefore, we investigated the Stat3/5 expression levels in each treated CTL and found that, in both gene and protein expression levels, the estrogen-induced suppression of Stat3/5 and the restoring efficacy of those by fulvestrant (Fig. 4i and Fig. S10).

These observations suggest that estrogen eliminates the self-activating ability of CTLs by depressing their Stat3/5-mediated IL-2 production at the transcriptional level, whereas anti-

estrogenic therapy can inhibit its immunosuppression and induce CTLs' proliferation and activation, resulting in anti-tumor effects on ERα-negative cancers.

Anti-estrogenic therapy affords drastic tumor reduction when combined with ICI by improving the TME

Tumor progression and the efficacy of all treatments, including ICI, are strongly influenced by the composition and abundance of immune cells within the TME [14, 35]. Numerous human studies, including patients with colorectal, breast, renal, skin, and lung cancer, have shown the significance of tumor-infiltrating lymphocytes as predictors of response to cancer treatment and overall survival [36]. In particular, the role of CTL, the final effector cells for cancer cells, is crucial regardless of the cause of therapeutic resistance. Indeed, it has been reported that CTLs were significantly associated with response to ICI in melanoma and urothelial cancer [37]. In also gastric cancer, CTLs were associated with an increased response probability [37]. Given the action of anti-estrogenic therapy against CTL within TME, we explored whether fulvestrant contributes to ICI efficacy. Of note, ERα-negative tumors (4T1 and CT26) completely refractory to ICIs such as anti-CTLA-4 and anti-PD-1 antibodies showed dramatic tumor regression by combining with fulvestrant administration (Fig 5a, b). Consistent with fulvestrant, tamoxifen or anastrozole combined with an anti-CTLA-4 antibody also showed remarkable anti-tumor effects (Fig. S11a, b). Among these consequences, CT26 treated with the

combination of fulvestrant and anti-CTLA-4 antibody was particularly interesting because the therapy completely suppressed tumor progression, and the tumor disappeared in some mice (Fig. 5a).

Most recently, as the most effective immunotherapy against cancer is the combination of anti-CTLA-4 antibody and anti-PD-1 antibody [38], we investigated how much the additional fulvestrant administration would have synergistic anti-tumor effects. The triple-drug therapy delayed the TNBC tumor growth to approximately one-fourth that of the untreated group and increased activated-T cells, especially activated-$CD8^+$ T cells, in the tumor by over ten-fold that of the untreated group (Fig 5c, d). These results overall represent the notion that estrogen creates an immunosuppressive TME, and its inhibitors can break the suppression, resulting in tumors acquiring sensitivity to ICIs by activating the T cells within ERα-negative tumors. Our discovery can be a novel strategy to overcome therapeutic resistance by augmenting T cell immunity to eliminate cancer cells.

Finally, assuming an actual clinical setting [39], we evaluated the therapeutic effects when fulvestrant was added to the combination of chemotherapy and immunotherapy used as a treatment for TNBC patients. While the 4T1 tumor used in this experiment was never responsive against paclitaxel monotherapy [14], a significant anti-tumor effect was obtained in combination with fulvestrant (Fig. 6a). In addition, the combination of paclitaxel and fulvestrant plus two kinds of ICI resulted in further dramatic tumor regressions (Fig. 6a). When we

confirmed intra-tumoral immune cells, T cells accompanied by activated phenotype, especially activated-$CD8^+$ T cells, were remarkably increased in tumors with fulvestrant treatment (Fig. 6b).

Discussion

In this study, we have demonstrated for the first time that estrogen is an immunomodulator that limits CTLs functions via suppression of IL-2 signal in CTL, enhancing tumor progression even if cancer cell does not express ERα. Although this sex steroid hormone is constantly and abundantly generated under noncancerous conditions in healthy bodies of premenopausal women and contributes to maintaining femininity, under cancerous conditions, its local and sustained action on not tumor cells but immune cells in the tumor makes TME fully immunosuppressive, resulting in accelerates tumor growth. On the other hand, anti-estrogenic therapy improved TME via inducing increment and activation of CTLs, reducing tumor progression in a tumor cell ERα-independent manner. It was of particular interest that, furthermore, a combination of immunotherapy represented by ICIs and anti-estrogenic therapy drastically slowed tumor growth even in ICI-resistant ERα-negative cancers.

While ICIs brought about a paradigm shift in systemic cancer therapy from conventional cytotoxic therapies, only some cancer patients respond markedly to ICIs, and most tumors show therapeutic resistance from the outset or will acquire it after the initial response [21]. The mechanisms that cause therapeutic resistance can be broadly distinguished into two types; one is intrinsic mechanisms, which are stemmed from specific genetic characteristics within cancer cells, and another one is extrinsic mechanisms, which are arisen from surrounding circumstances such as cytokines and stromal cells [40]. Recent medical development shows the

importance of extrinsic mechanisms in therapeutic resistance acquisition [41]. Indeed, ICI effectiveness is strongly suppressed by various extrinsic immunosuppressive elements of each step in the anti-tumor immunity cycle [40, 41]. For instance, immunosuppressive cells such as tumor-associated macrophages, regulatory T cells, and MDSCs are critical factors that contribute to acquiring therapeutic resistance [41]. Furthermore, cytokines secreted by these immunosuppressive and tumor cells also create and augment the tumor progression and immune escape of cancers [41]. Therefore, numerous studies targeting immunosuppressive cells aimed to release therapeutic resistance are ongoing worldwide, and some approaches have successfully sensitized ICI-resistant tumors in preclinical models [42, 43].

Nevertheless, those preclinical findings have never been well-translated to the clinical arena so far. We attribute this to the complexity of the TME and therapeutic resistant-acquiring mechanisms in spontaneous human cancers. The successful clinical application requires either understanding entirely the mechanisms underlying resistance or a direct and robust driving of the final effector cells of adaptive immunity, CTLs [44]. Of note, since the anti-estrogenic therapy we proposed in this study directly acts on CTL, it may improve TME and reverse the resistance regardless of the mechanisms of therapeutic resistance acquisition. In fact, the administration of fulvestrant, tamoxifen, or anastrozole sensitized ICI-insusceptible tumors and elicited dramatic anti-tumor effects when combined with ICI.

As the therapeutic mechanisms, we elucidated that, within the tumors, anti-estrogenic therapy reversed estrogen-derived direct suppression of CTL, in which estrogen suppresses IL-2 production from CTL and brings the loss of an autocrine action caused by IL-2. Intra-tumoral CTLs have been known as a factor that positively correlated with the response to ICI in various cancers [37, 44]. Besides, the proliferation of effector T cells, including CTLs, has been positively regulated by STAT3/5-mediated IL-2 production [34, 45]. Under diverse situations, IL-2 influences effector T cell differentiation and determines the fate of antigen receptor-activated T cells [33]. When acute viral infection occurs, CTL expansion is three-fold lower in IL-2-deficient mice than in the wild type, resulting in notable repression of viral clearance by virus-specific CTLs [45]. Also in cancers, it has been reported that the expansion of the antigen-specific CTL population is two- to five-fold lower in IL-2 receptor-deficient mice than in the wild-type [46]. Contrary to this, when CTLs expose to high concentrations of IL-2, they proliferate vigorously [47]. Of note, however, IL-2 is not expressed or expressed at low concentrations in tumor tissue [48]. Given these contexts, our data that estrogen suppresses intra-tumoral CTL via inhibiting the autocrine IL-2 production and the resultant induced ICI resistance appears sufficiently convincing.

Nowadays, immunohistochemical examination of ERα in breast cancer cells harvested by a biopsy or surgery has been routinely conducted to select patients who would treat with hormonal therapy [30]. As a result, only ERα-positive breast cancer patients are treated with

anti-estrogenic therapy, one of the hormonal therapies [30]. On the other hand, TNBC patients cannot be managed with anti-estrogenic therapy because TNBC lacks ERα expression; hence, chemotherapy is the only treatment option [35]. It has also recently become clear that ERβ and GPER1 are expressed even in some TNBC cases and act tumor-suppressively via estrogen binding [26]. In particular, it has been reported that ERβ is also expressed in immune cells and promotes B cell proliferation [49]. Still, its expression in CTLs, which we focused on in this study, is lower than ERα, and the details of how important this is are not yet known [50]. In our paper, ERβ and GPER1 were excluded from the detailed analyses because they did not contribute to TNBC prognosis, but we believe that a thorough investigation of these targets is also warranted for future medical development. Needless to say, other cancers besides ERα-positive breast cancer, including colon and skin cancer, are also not eligible for anti-estrogen therapy. However, from now on, it is necessary to note that estrogen not only acts directly on cancer cells but also on immune cells in TME. In other words, anti-estrogenic therapy may be used for all cancer types accompanied by immune cell infiltration. In particular, as our data indicate, the treatment may be more effective for cancers with high CTL invasion.

Despite growing evidence implicating estrogen as a fundamental mediator in numerous diseases [1, 5], its potential role in anti-tumor immune responses in cancer patients without estrogen sensitivity of tumor cells has hitherto been almost unknown. The present study clarified that estrogen action in TME can affect cancer progression independently of ERα

expression on cancer cells, in other words, mediating CTLs directly. In addition, we proved that the blocking of estrogen signals is a promising therapy to improve the efficacy of ICI and reverse immune resistance. Advances in research and development of this therapeutic strategy may expand the reach of immunotherapy to more various types of cancer and allow more patients to benefit.

Conclusions

Taken together, we show that anti-estrogenic therapies, including ER antagonists, have the potential to maximize the therapeutic efficacy of cancer immunotherapy regardless of tumor cells' ERα expression, requiring further translational research of this therapeutic strategy to transfer into clinical application.

List of abbreviations

Tumor microenvironment: TME

Cytotoxic T lymphocyte: CTL

Immune checkpoint inhibitor: ICI

Estrogen receptor: ER

Triple-negative breast cancer: TNBC

Mitogen-activated protein kinase: MAPK

Phosphoinositide 3-kinase: PI3K

Myeloid-derived suppressor cell: MDSC

G protein-coupled estrogen receptor 1: GPER1

Materials and methods

Human clinical data analysis

Gene expression data and clinical data of HSD17B1, CYP19A1, ESR2, or GPER in the "Breast Invasive Carcinoma (TCGA, PanCancer Atlas)" dataset (N=1083) were obtained from www.cbioportal.org. We assigned these samples to breast cancer subtypes based on the PAM50 classification and extracted only TNBC patients' data (N=171). Then we generated scatter plots of the expression correlation of the HSD17B1 or CYP19A1 gene and each effector T cell marker gene (PRF1, GZMB, IFNG, CD3E, CD69, and CD8A), each myeloid cell-related gene (CD11b, CD14, CD15, CD163, CD206, CD209) and calculated the Spearman correlation coefficient between the two genes. TIMER2.0 web server, which provides a more robust estimation of immune infiltration levels for TCGA using state-of-the-art algorithms, revealed the association between HSD17B1, ESR2, or GPER gene expression and $CD8^+$ T cell subset abundance within tumors. We generated bar graphs to compare $CD8^+$ T cell infiltration levels within tumors in TNBC patients with low (bottom 50 %) or high (top 50 %) HSD17B1 gene expression. Finally, we evaluated the effects of HSD17B1, ESR2, or GPER gene expression on TNBC patients' clinical outcomes by generating the Kaplan-Meier survival curve. Data with missing some clinical information were excluded from these analyses.

Cell lines

Mouse TNBC cell line 4T1 and human ER-positive breast cancer cell line T47D were purchased from the American Type Culture Collection, and mouse colon cancer cell line CT26 was kindly provided by Dr. Hidemitsu Kitamura, Hokkaido University. T47D, 4T1, and CT26 cell lines were maintained in RPMI-1640 (Fujifilm Wako Pure Chemical Corporation). Culture media was supplemented with 10 % fetal bovine serum (FBS) (Sigma-Aldrich), 100 U/ml penicillin (Nacalai Tesque), 100 μg/ml streptomycin (Nacalai Tesque), 0.1 mM MEM nonessential amino acids (Nacalai Tesque), and maintained at 37 °C with 5 % CO_2. Mycoplasma contamination of cell lines was checked using the MycoAlert® Mycoplasma Detection Kit (Lonza Group), according to the manufacturer's instructions; no contamination was found.

Protein expression analysis

Protein expression analysis for ERα in 4T1, CT26, and T47D (positive control) cell lines and STAT3 and 5 in $CD8^+$ T cells was performed by Western blotting. Cell lysates were obtained from each cell line by lysing in RIPA buffer (Nacalai Tesque) and centrifuged to collect a supernatant sample. Then we added a 4×SDS sample buffer (Sigma-Aldrich) to each supernatant sample and boiled them at 100 °C. Protein was separated by electrophoretic migration at 200 V using a 10 % acrylamide gel and transferred to a polyvinylidene difluoride membrane at 25 V. The membrane was blocked with 3 % skim milk in TBS-T at room temperature, then probed with 1:500 dilution of anti-ERα antibody (#MA1-80216, Thermo

Fisher Scientific), 1:1000 dilution of anti-STAT3 antibody (#9139S, Cell Signaling Technology), or anti-STAT5 antibody (#94205S, Cell Signaling Technology) at 4 °C overnight with gentle shaking, followed by incubation in 1:1000 dilution of horseradish peroxidase (HRP)-linked anti-mouse IgG antibody (#405306, BioLegend) or HRP-linked anti-rabbit IgG antibody (#7074S, Cell Signaling Technology) at room temperature. Proteins were visualized using Super Signal West Femto Maximum Sensitivity Substrate (Thermo Fisher Scientific). As an internal control molecule, we detected HPRT or ACTB using anti-HPRT antibody (#15059-1-AP, Proteintech) or anti-βactin antibody (#3700S, Cell Signaling Technology), respectively.

Cell proliferation assay

The cell proliferation of 4T1, CT26, and T47D (positive control) cell lines was assessed by the MTT assay using MTT Cell Count Kit (Nacalai Tesque). Cells were seeded at a density of 3×10^3 in a 96-well plate and stimulated with varying concentrations (1 nM-1 μM) of 17β-Estradiol (E2, Nacalai Tesque). The cell proliferation was followed up for 3 days. Absorbance at a test wavelength of 570 nm and a reference wavelength of 650 nm was measured using a MULTISKAN FC (Thermo Fisher Scientific).

Mouse tumor model experiment

Six to seven weeks old female BALB/c (including wild and nude) mice were purchased from Japan SLC and Jackson Laboratory, respectively. The mice were maintained under specific pathogen-free conditions and housed in 12 hours light/12 hours dark cycle in the animal facility at Hokkaido University and used in the experiment at eight weeks old, which reached sexual maturity. For *in vivo* assay, 1 or 2×10^5 tumor cells were inoculated subcutaneously into the right flank of syngeneic female mice and grouped randomly on day 5. Fulvestrant (FUL, 1.25 mg/3 days, Tokyo Chemical Industry), E2 (10 μg/day, Nacalai Tesque), tamoxifen (TAM, 1 mg/day, Nacalai Tesque), anastrozole (ANZ, 1 mg/day, AstraZeneca), anti-IL-2 antibody (200 μg/4 days, BioLegend), anti-PD-1 antibody (250 μg/3 days, BioXCell), or anti-CTLA-4 antibody (250 μg/3 days, BioXCell) was intraperitoneally administered when tumor size reached 5 mm in diameter. Anti-CD8 antibody (100 μg/injection, BioLegend) was intraperitoneally administered the day before and six days before tumor inoculation. Tumor size was measured by a caliper three times a week. A week after E2 administration started, blood was collected, and E2 concentration in serum was measured by NIKKEN SEIL, Japan (achieved blood concentration of E2: 126-359 pg/ml). The tumors and uterus were collected 14 days after the cell inoculation or development, measured each tumor weight and uterine weight, followed by the isolation of tumor-infiltrating immune cells from solid tumors. The Animal Care Committee of Hokkaido University approved all animal experiments (Approval number: 19-0094).

Mouse ovariectomy model experiment

A week before tumor inoculation, female BALB/c mice were ovariectomized or sham-operated. Briefly, mice were anesthetized, both the right and left flank were shaved with an electronic razor, and the skin was sterilized with alcohol. Then we made an incision on the skin and muscle wall and externalized and excised the ovary. For sham operation, the ovary was externalized and then returned internally. After excision, the muscle wall and skin were sutured, respectively, then recovered from anesthesia.

Isolation of tumor-infiltrating immune cells from solid tumor

Isolation of tumor-infiltrating immune cells from solid tumors was performed by using BD Horizon Dri Tumor and Tissue Dissociation Reagent (BD Biosciences) according to the manufacturer's instructions. The recovered tumor-infiltrating immune cells were used as samples for flow cytometry or RNA extraction.

Analysis of tumor-infiltrating immune cells

Tumor-infiltrating immune cells from solid tumors were analyzed by flow cytometry. For extracellular staining, cells were washed and blocked with FcR Blocking Reagent (BioLegend) and stained with 4',6-diamidino-2-phenylindole (Cayman Chemical Company) and the antibodies against the following molecules; CD3ε, CD4, CD8α, CD11b, CD45, CD69, CD86,

CD206, F4/80, Ly6C, and Ly6G (BioLegend). For intracellular staining, cells were fixed and permeabilized with Cytofix/Cytoperm™ Buffer (BD Biosciences) after extracellular staining, then intracellular IFNγ was stained (BioLegend). Data were acquired using FACSCelesta flow cytometer (BD Biosciences) and analyzed using FlowJo software (BD Biosciences). The gating strategies were as follows; first selected live cells based on forward- and side-scatters, with subsequent selection of singlets. When analyzing immune cells, $CD45^+$ cells were gated, then a target population was expanded.

Gene expression analysis

Gene expression was analyzed by reverse transcription-polymerase chain reaction (RT-PCR). Total RNA was extracted using TRIsure reagent (NIPPON Genetics). cDNA was synthesized from extracted RNA using ReverTra Ace® qPCR RT Master Mix (TOYOBO). PCR was performed on cDNA using KAPA SYBR® FAST qPCR Kit Master Mix (2X) ABI Prism™ (NIPPON Genetics) on a StepOnePlus Real-Time PCR System (Thermo Fisher Scientific). Glyceraldehyde-3-phosphate dehydrogenase gene (*Gapdh*) expression was used as an internal control, and the expression levels of each target gene were normalized to *Gapdh*. The corresponding primers were as follows:

Gapdh: Fw-TCAAATGGGGTGAGGCCGGT, Rv-TTGCTGACAATCTTGAGTGA

Gzmb: Fw-ACTCTTGACGCTGGGACCTA, Rv-AGTGGGGCTTGACTTCATGT

Prf1: Fw-TCATCATCCCAGCCGTAGT, Rv-ATTCATGCCAGTGTGAGTGC

Ifng: Fw-AAGACAATCAGGCCATCAGCA, Rv-AGCGACTCCTTTTCCGCTTC

Il2: Fw-AGATGAACTTGGACCTCTGCG, Rv-AAAGTCCACCACAGTTGCTG

Esr2: Fw-CTGTGCCTCTTCTCACAAGGA, Rv-TGCTCCAAGGGTAGGATGGAC

Gper: Fw-GCCACATAGTCAACCTTGCAGC, Rv-CGTCTTCTGCTCCACATAGAGC

CTLs stimulation assay

Splenocytes were isolated from the spleen of female BALB/c mice and depleted of red blood cells with ACK lysis buffer (Thermo Fisher Scientific). Mouse CTLs (=$CD8^+$ T cells) were sorted from mouse splenocytes using mouse CD8α MicroBeads (Miltenyi Biotec) in the magnetic-activated cell sorting (MACS) system. Human CTLs were isolated from human mononuclear cells (Sigma-Aldrich) by the MACS system. CTLs were seeded at a density of 2×10^5 in a 96-well plate and stimulated with anti-CD3ε (1 μg/well) and anti-CD28 (2 μg/well) antibodies (BioLegend) plus varying concentrations of E2 (10 nM-1 μM) and FUL (10 μM). For wells that do not contain E2 or FUL, equal volumes of DMSO were added. Cultured CTLs were collected on day 4 and analyzed by flow cytometry or used as samples for RNA extraction. The production of IL-2 from CTLs cultured with DMSO or E2 with/without FUL was measured by the enzyme-linked immunosorbent assay (ELISA) using LEGEND MAX Mouse IL-2 ELISA Kit (BioLegend).

Gene ontology enrichment analysis

The total extracted RNA of CTLs treated with DMSO or E2 or E2 plus FUL was analyzed by RNA sequencing analysis (RNA-seq). RNA-seq was performed at Kazusa DNA Research Institute, Japan. Gene ontology enrichment analysis of the generated datasets of differentially expressed genes was performed using the ShinyGO 0.76.2 bioinformatics graphical web application (http://bioinformatics.sdstate.edu/go/) based on gene lists obtained from RNA-seq. The T cell activation genes obtained from the PANTHER Pathways dataset were used as the background, and the top 10 with higher gene enrichment scores were shown. In fig.4h, the upper graphic represents downregulated pathway by E2 treatment, and the bottom one represents upregulated pathway by FUL treatment. Gene expression levels of signal transducer and activator of transcription (Stat) 3, 5a, and 5b were represented using RNA-seq outcome.

Statistical analysis

Sample size and statistical tests are described in the figure legends. Every series of data are shown as mean ± SEM. A two-sided Student's *t*-test was used to compare the two groups. One-way ANOVA with the Tukey-Kramer test was used to compare the three or more groups. The survival curves of TNBC patients and mice were determined using the Kaplan-Meier method, and the Log-rank test was used for statistical evaluation. Spearman correlation coefficient was

used to examine the correlation between the two indicators. The p-value of < 0.05 was considered to be statistically significant. All statistical analyses were performed with JMP® Pro 16 software (SAS Institute).

Declarations

Ethics approval and consent to participate

All animal procedures were approved by the Animal Care Committee of Hokkaido University (Approval number: 19-0094).

Consent for publication

Not applicable.

Data availability

Data are available on reasonable request. The datasets used and/or analyzed during the current study are available from the corresponding author.

Conflict of interest statement

The authors have declared that no conflict of interest exists.

Funding

This work was partly supported by JST SPRING (#JPMJSP2119, N. Kajihara) and JSPS KAKENHI (#22J21076, N. Kajihara).

Authors' contributions

NK and KS designed the study. NK and YG performed experiments. All authors analyzed data and discussed the results. NK and KS contributed to manuscript preparation. All authors approved the final version of this manuscript for publication.

Acknowledgements

The authors thank Tomoki Murata, Masafumi Tanji, Nanumi Han, Haruka Wada, and Yoshinori Hasegawa for their helpful discussions and advice, and technical assistance with part of some experiments.

References

[1] Chen C, Gong X, Yang X, Shang X, Du Q, Liao Q, et al. The roles of estrogen and estrogen receptors in gastrointestinal disease (Review). Oncol Lett. 2019;18:5673–80.

[2] Tohyama S, Ogino Y, Lange A, Myosho T, Kobayashi T, Hirano Y, et al. Establishment of estrogen receptor 1 (ESR1)-knockout medaka: ESR1 is dispensable for sexual development and reproduction in medaka, Oryzias latipes. Dev Growth Differ. 2017;59:552–61.

[3] Gompel A. Hormone and breast cancer. Presse Medicale. 2019;48:1085–91.

[4] Lin CY, Ström A, Vega VB, Kong SL, Yeo AL, Thomsen JS, et al. Discovery of estrogen receptor alpha target genes and response elements in breast tumor cells. Genome Biol. 2004;5.

[5] Cunningham M, Gilkeson G. Estrogen Receptors in Immunity and Autoimmunity. Clin Rev Allergy Immunol. 2011;40:66–73.

[6] Wang T, Jin J, Qian C, Lou J, Lin J, Xu A, et al. Estrogen/ER in anti-tumor immunity regulation to tumor cell and tumor microenvironment. Cancer Cell Int. 2021;21:1–13.

[7] Chuffa LG de A, Lupi-Júnior LA, Costa AB, Amorim JP de A, Seiva FRF. The role of sex hormones and steroid receptors on female reproductive cancers. Steroids. 2017;118:93–108.

[8] Hsieh CC, Trichopoulos D, Katsouyanni K, Yuasa S. Age at menarche, age at menopause, height and obesity as risk factors for breast cancer: Associations and interactions in an international case-control study. Int J Cancer. 1990;46:796–800.

[9] Zattarin E, Leporati R, Ligorio F, Lobefaro R, Vingiani A, Pruneri G, et al. Hormone Receptor Loss in Breast Cancer: Molecular Mechanisms, Clinical Settings, and Therapeutic Implications. Cells. 2020;9:2644.

[10] Morgan DAL, Refalo NA, Cheung KL. Strength of ER-positivity in relation to survival in ER-positive breast cancer treated by adjuvant tamoxifen as sole systemic therapy. Breast. 2011;20:215–9.

[11] Braun L, Mietzsch F, Seibold P, Schneeweiss A, Schirmacher P, Chang-Claude J, et al. Intrinsic breast cancer subtypes defined by estrogen receptor signalling-Prognostic relevance of progesterone receptor loss. Modern Pathology. 2013;26:1161–71.

[12] Backes FJ, Walker CJ, Goodfellow PJ, Hade EM, Agarwal G, Mutch D, et al. Estrogen receptor-alpha as a predictive biomarker in endometrioid endometrial cancer. Gynecol Oncol. 2016;141:312–7.

[13] Deepak KGK, Vempati R, Nagaraju GP, Dasari VR, Nagini S, Rao DN, et al. Tumor microenvironment: Challenges and opportunities in targeting metastasis of triple negative breast cancer. Pharmacol Res. 2020;153:104683.

[14] Kajihara N, Kobayashi T, Otsuka R, Nio J, Tomohiro K. Tumor - derived interleukin-34 creates an immunosuppressive and chemoresistant tumor microenvironment by modulating myeloid-derived suppressor cells in triple-negative breast cancer. Cancer Immunol Immunother. 2023;72:851–64.

[15] Hangai S, Kawamura T, Kimura Y, Chang CY, Hibino S, Yamamoto D, et al. Orchestration of myeloid-derived suppressor cells in the tumor microenvironment by ubiquitous cellular protein TCTP released by tumor cells. Nat Immunol. 2021;22:947–57.

[16] Márquez-Garbán DC, Deng G, Comin-Anduix B, Garcia AJ, Xing Y, Chen HW, et al. Antiestrogens in combination with immune checkpoint inhibitors in breast cancer immunotherapy. J Steroid Biochem Mol Biol. 2019;193:105415.

[17] Chakraborty B, Byemerwa J, Shepherd J, Haines CN, Baldi R, Gong W, et al. Inhibition of estrogen signaling in myeloid cells increases tumor immunity in melanoma. J Clin Invest. 2021;131:1–16.

[18] Salem ML. Estrogen, a double-edged sword: Modulation of TH1- and TH2-mediated inflammations by differential regulation of TH1/TH2 cytokine production. Curr Drug Targets Inflamm Allergy. 2004;3:97–104.

[19] Nakamura N, Miyazaki K, Kitano Y, Fujisaki S, Okamura H. Suppression of cytotoxic T-lymphocyte activity during human pregnancy. J Reprod Immunol. 1993;23:119–30.

[20] Haghmorad D, Amini AA, Mahmoudi MB, Rastin M, Hosseini M, Mahmoudi M. Pregnancy level of estrogen attenuates experimental autoimmune encephalomyelitis in both ovariectomized and pregnant C57BL/6 mice through expansion of Treg and Th2 cells. J Neuroimmunol. 2014;277:85–95.

[21] Conforti F, Pala L, Bagnardi V, De Pas T, Martinetti M, Viale G, et al. Cancer immunotherapy efficacy and patients' sex: a systematic review and meta-analysis. Lancet Oncol. 2018;19:737–46.

[22] Svoronos N, Perales-Puchalt A, Allegrezza MJ, Rutkowski MR, Payne KK, Tesone AJ, et al. Tumor cell–independent estrogen signaling drives disease progression through mobilization of myeloid-derived suppressor cells. Cancer Discov. 2017;7:72–85.

[23] Grumbach MM, Auchus RJ. Estrogen: Consequences and implications of human mutations in synthesis and action. J Clin Endocrinol Metab. 1999;84:4677–94.

[24] Wu AH, Seow A, Arakawa K, Van Den Berg D, Lee HP, Yu MC. HSD17B1 and CYP17 polymorphisms and breast cancer risk among Chinese women in Singapore. Int J Cancer. 2003;104:450–7.

[25] Setiawan VW, Hankinson SE, Colditz GA, Hunter DJ, De Vivo I. HSD17B1 Gene Polymorphisms and Risk of Endometrial and Breast Cancer. Cancer Epidemiol Biomarkers Prev. 2004;13:213–9.

[26] Treeck O, Schüler-Toprak S, Ortmann O. Estrogen Actions in Triple-Negative Breast Cancer. Cells. 2020;9.

[27] Howell SJ, Johnston SRD, Howell A. The use of selective estrogen receptor modulators and selective estrogen receptor down-regulators in breast cancer. Best Pract Res Clin Endocrinol Metab. 2004;18:47–66.

[28] Tang H, Liao Y, Zhang C, Chen G, Xu L, Liu Z, et al. Fulvestrant-mediated inhibition of estrogen receptor signaling slows lung cancer progression. Oncol Res. 2014;22:13–20.

[29] Mishra AK, Abrahamsson A, Dabrosin C. Fulvestrant inhibits growth of triple negative breast cancer and synergizes with tamoxifen in ERα positive breast cancer by up-regulation of ERβ. Oncotarget. 2016;7:56876–88.

[30] Lumachi F, Brunello A, Maruzzo M, Basso U, Basso S. Treatment of Estrogen Receptor-Positive Breast Cancer. Curr Med Chem. 2013;20:596–604.

[31] Ross SH, Cantrell DA. Signaling and Function of Interleukin-2 in T Lymphocytes. Annu Rev Immunol. 2018;36:411–33.

[32] Feau S, Arens R, Togher S, Schoenberger SP. Autocrine IL-2 is required for secondary population expansion of CD8 + memory T cells. Nat Immunol. 2011;12:908–13.

[33] Dai Z, Konieczny BT, Lakkis FG. The Dual Role of IL-2 in the Generation and Maintenance of CD8 + Memory T Cells. J Immunol. 2000;165:3031–6.

[34] Johnston JA, Bacon CM, Finbloom DS, Rees RC, Kaplan D, Shibuya K, et al. Tyrosine phosphorylation and activation of STAT5, STAT3, and Janus kinases by interleukins 2 and 15. Proc Natl Acad Sci USA. 1995;92:8705–9.

[35] Kajihara N, Kitagawa F, Kobayashi T, Wada H, Otsuka R, Seino KI. Interleukin-34 contributes to poor prognosis in triple-negative breast cancer. Breast Cancer. 2020;27:1198–204.

[36] Balkwill FR, Capasso M, Hagemann T. The tumor microenvironment at a glance. J Cell Sci. 2012;125:5591–6.

[37] Liu R, Yang F, Yin JY, Liu YZ, Zhang W, Zhou HH. Influence of Tumor Immune Infiltration on Immune Checkpoint Inhibitor Therapeutic Efficacy: A Computational Retrospective Study. Front Immunol. 2021;12:1–15.

[38] Chapman PB, Jayaprakasam VS, Panageas KS, Callahan M, Postow MA, Shoushtari AN, et al. Risks and benefits of reinduction ipilimumab/nivolumab in melanoma patients previously treated with ipilimumab/nivolumab. J Immunother Cancer. 2021;9:1–6.

[39] Kagihara JA, Andress M, Diamond JR. Nab-paclitaxel and atezolizumab for the treatment of PD-L1-positive, metastatic triple-negative breast cancer: review and future directions. Expert Rev Precis Med Drug Dev. 2020;5:59–65.

[40] Zhao X, Subramanian S. Intrinsic resistance of solid tumors to immune checkpoint blockade therapy. Cancer Res. 2017;77:817–22.

[41] Tie Y, Tang F, Wei Y quan, Wei X wei. Immunosuppressive cells in cancer: mechanisms and potential therapeutic targets. J Hematol Oncol. 2022;15:61.

[42] Guan X, Polesso F, Wang C, Sehrawat A, Hawkins RM, Murray SE, et al. Androgen receptor activity in T cells limits checkpoint blockade efficacy. Nature. 2022;606:791–6.

[43] Hama N, Kobayashi T, Han N, Kitagawa F, Kajihara N, Otsuka R, et al. Interleukin-34 Limits the Therapeutic Effects of Immune Checkpoint Blockade. iScience. 2020;23:101584.

[44] Sade-Feldman M, Yizhak K, Bjorgaard SL, Ray JP, de Boer CG, Jenkins RW, et al. Defining T Cell States Associated with Response to Checkpoint Immunotherapy in Melanoma. Cell. 2018;175:998-1013.e20.

[45] Boyman O, Sprent J. The role of interleukin-2 during homeostasis and activation of the immune system. Nat Rev Immunol. 2012;12:180–90.

[46] Mitchell DM, Ravkov E V., Williams MA. Distinct Roles for IL-2 and IL-15 in the Differentiation and Survival of CD8+ Effector and Memory T Cells. J Immunol. 2010;184:6719–30.

[47] Cho JH, Boyman O, Kim HO, Hahm B, Rubinstein MP, Ramsey C, et al. An intense form of homeostatic proliferation of naive CD8+ cells driven by IL-2. J Exp Med. 2007;204:1787–801.

[48] Sun Z, Ren Z, Yang K, Liu Z, Cao S, Deng S, et al. A next-generation tumor-targeting IL-2 preferentially promotes tumor-infiltrating CD8+ T-cell response and effective tumor control. Nat Commun. 2019;10:3874.

[49] Kovats S. Estrogen receptors regulate innate immune cells and signaling pathways. Cell Immunol. 2015;294:63–9.

[50] Phiel KL, Henderson RA, Adelman SJ, Elloso MM. Differential estrogen receptor gene expression in human peripheral blood mononuclear cell populations. Immunol Lett. 2005;97:107–13.

Figure 1: Potential involvement of estrogen-inducible enzyme HSD17B1 with immunity in human TNBC.

(a) Spearman correlation coefficient between relative HSD17B1 and PRF1, GZMB, IFNG, CD3E, CD69, and CD8A expression in TNBC tumors are shown (n=159). (b) Spearman correlation coefficient between relative HSD17B1 expression in tumors and intra-tumoral $CD8^+$ T cell infiltration is shown. (c) Bar graphs represent $CD8^+$ T cell infiltration in TNBC tumors stratified to HSD17B1 high and HSD17B1 low by median expression. (d) Kaplan-Meier plot of overall survival of TNBC patients with high or low HSD17B1 expression. Values were analyzed by a two-sided Student's *t*-test (c) and a Log-rank test (d) and are shown as mean±SEM (c).

Figure 2: Effects of estrogen on tumor growth and survival in ERα-negative cancers.

(a) Western blotting of ERα in 4T1 and CT26 cell lines. ERα-positive T47D cell line served as a positive control. (b) Bar graphs represent cell proliferation of 4T1 and CT26 cells at varying concentrations of E2 that were measured by MTT assay for three days (n=3). (c) Subcutaneous tumor growth in BALB/c sham-operated (Sham) or ovariectomized (OVX) mice inoculated with 4T1 or CT26 cells and supplemented with dimethyl sulfoxide (DMSO) or E2 ($1x10^5$ cells, n=4-6). *P*-values are shown as of day 14. (d) Kaplan-Meier plot of overall survival in BALB/c Sham or OVX mice inoculated with 4T1 cells and supplemented with DMSO or E2 (n=6). (e)

Subcutaneous tumor growth in BALB/c nu/nu Sham or OVX mice inoculated with 4T1 cells ($1x10^5$ cells, n=3). *P*-values are shown as of day 14. Values were analyzed by a Tukey-Kramer test (b, c), a Log-rank test (d), and a two-sided Student's *t*-test (e) and are shown as mean±SEM (b, c, e).

Figure 3: Effects of ER antagonist (fulvestrant) on ERα-negative tumor growth and tumor microenvironment.

(a) Subcutaneous tumor growth in BALB/c mice inoculated with 4T1 or CT26 cells ($1x10^5$ cells, n=6-8) and treated with dimethyl sulfoxide (DMSO) or fulvestrant (FUL). Similar results were obtained in several independent experiments. (b-e) 4T1 cells ($1x10^5$ cells) were subcutaneously inoculated into BALB/c mice. DMSO or FUL was administered intraperitoneally once per three days from day 5 to day 14. (b) Bar graphs represent the frequency of myeloid-derived suppressor cells (MDSC, $CD11b^+Ly6C^{lo}Ly6G^+$ cells), macrophages (MΦ, $CD11b^+F4/80^+$ cells), and T cells ($CD3^+$ cells) within $CD45^+$ cells infiltrated in the 4T1 tumors (n=8). (c) Bar graphs represent the frequency of M1-MΦ ($CD69^+$ cells) and M2-MΦ ($CD206^+$ cells) within $CD11b^+F4/80^+$ cells infiltrated in the 4T1 tumors (n=8). (d) Bar graphs represent the frequency of $CD4^+$ T cells ($CD3^+CD4^+$ cells) and $CD8^+$ T cells ($CD3^+CD8^+$ cells) within $CD45^+$ cells infiltrated in the 4T1 tumors (n=8). (e) Bar graphs represent the gene expression of granzyme b (*Gzmb*), perforin 1 (*Prf1*), and interferon-gamma (*Ifng*) in 4T1 tumors (n=3). Gene expression

levels were determined by RT-PCR, as normalized to *Gapdh*. Values were analyzed by a two-sided Student's *t*-test and are shown as mean±SEM.

Figure 4: $CD8^+$ T cell-mediated mechanisms of anti-tumor effect by ER antagonist in ERα-negative cancer.

(a) Schematic of dimethyl sulfoxide (DMSO) or fulvestrant (FUL) treatment combined with anti-CD8 antibody (αCD8) or isotype control (IgG) in murine tumor implantation experiment. The timeline shows the procedure of tumor inoculation and antibody treatment. (b) Subcutaneous tumor growth in BALB/c mice inoculated with 4T1 cells ($1x10^5$ cells, n=3-4) and treated with DMSO or FUL and αCD8 or IgG. Bar graphs represent each group's tumor volume 14 days post tumor development. (c) $CD8^+$ T cells were isolated from human mononuclear cells and cultured with DMSO or E2 (1 μM) or E2 (1 μM) combined with FUL (10 μM) for 4 days. Bar graphs represent the frequency of $CD8^+$ and $CD8^+CD69^+$ T cells within $CD45^+$ cells (n=3). (d, e) $CD8^+$ T cells were isolated from murine splenocytes and cultured with DMSO or E2 (10 nM-1 μM) or E2 (1 μM) combined with FUL (10 μM) for 4 days. (d) Bar graphs represent the gene expression of interleukin-2 (*Il2*) in $CD8^+$ T cells cultured with DMSO or E2 (1 μM) or E2 (1 μM) combined with FUL (10 μM) for 4 days. (n=3). Gene expression levels were determined by RT-PCR, as normalized to *Gapdh*. (e) Bar graphs represent IL-2 concentration in supernatants of $CD8^+$ T cells cultured with DMSO or varying concentrations

of E2 (10 nM-1 μM) or E2 (1 μM) combined with FUL (10 μM) for 4 days (n=3). (f) Schematic of DMSO or FUL treatment combined with anti-IL-2 antibody (αIL-2) or IgG in murine tumor implantation experiment. The timeline shows the procedure of tumor inoculation and antibody treatment. (g) Subcutaneous tumor growth in BALB/c mice inoculated with 4T1 cells ($1x10^5$ cells, n=4) and treated with DMSO or FUL and αIL-2 or IgG. Bar graphs represent each group's tumor volume 14 days post tumor development. (h, i) $CD8^+$ T cells were isolated from murine splenocytes and cultured with DMSO or E2 (1 μM) or E2 (1 μM) combined with FUL (10 μM) for 4 days. (h) Gene ontology enrichment analysis of differentially expressed genes in $CD8^+$ T cells when each treatment. Pathways downregulated by E2 and upregulated by FUL are shown, respectively. (i) Bar graphs represent the gene expression of Stat3, Stat5a, and Stat5b in $CD8^+$ T cells when each treatment. Values were analyzed by a Tukey-Kramer test (b-e, g) and are shown as mean±SEM (b-e, g).

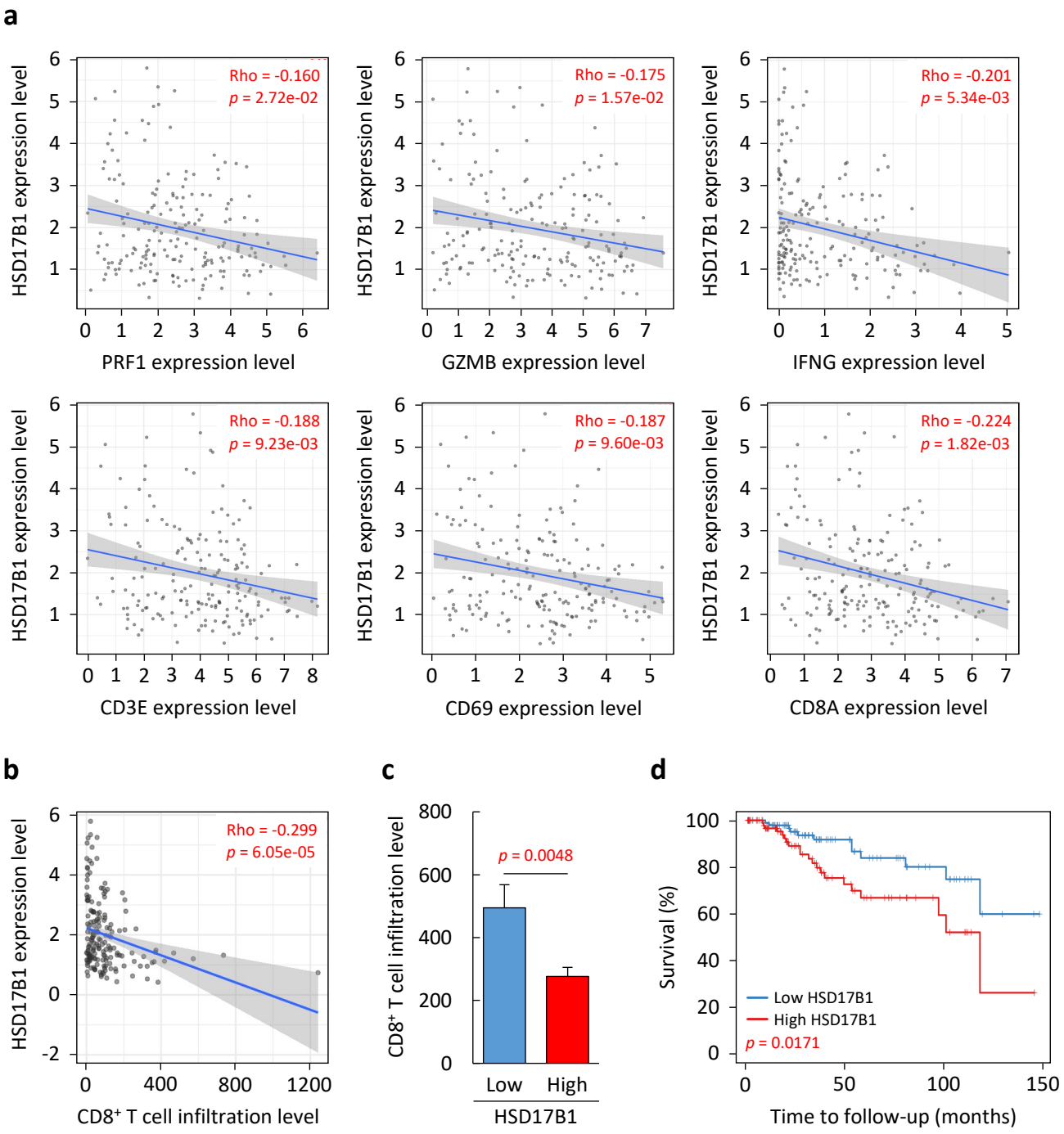
Figure 5: Effects of ER antagonist combined with immune checkpoint inhibitor on ERα-negative tumor growth.

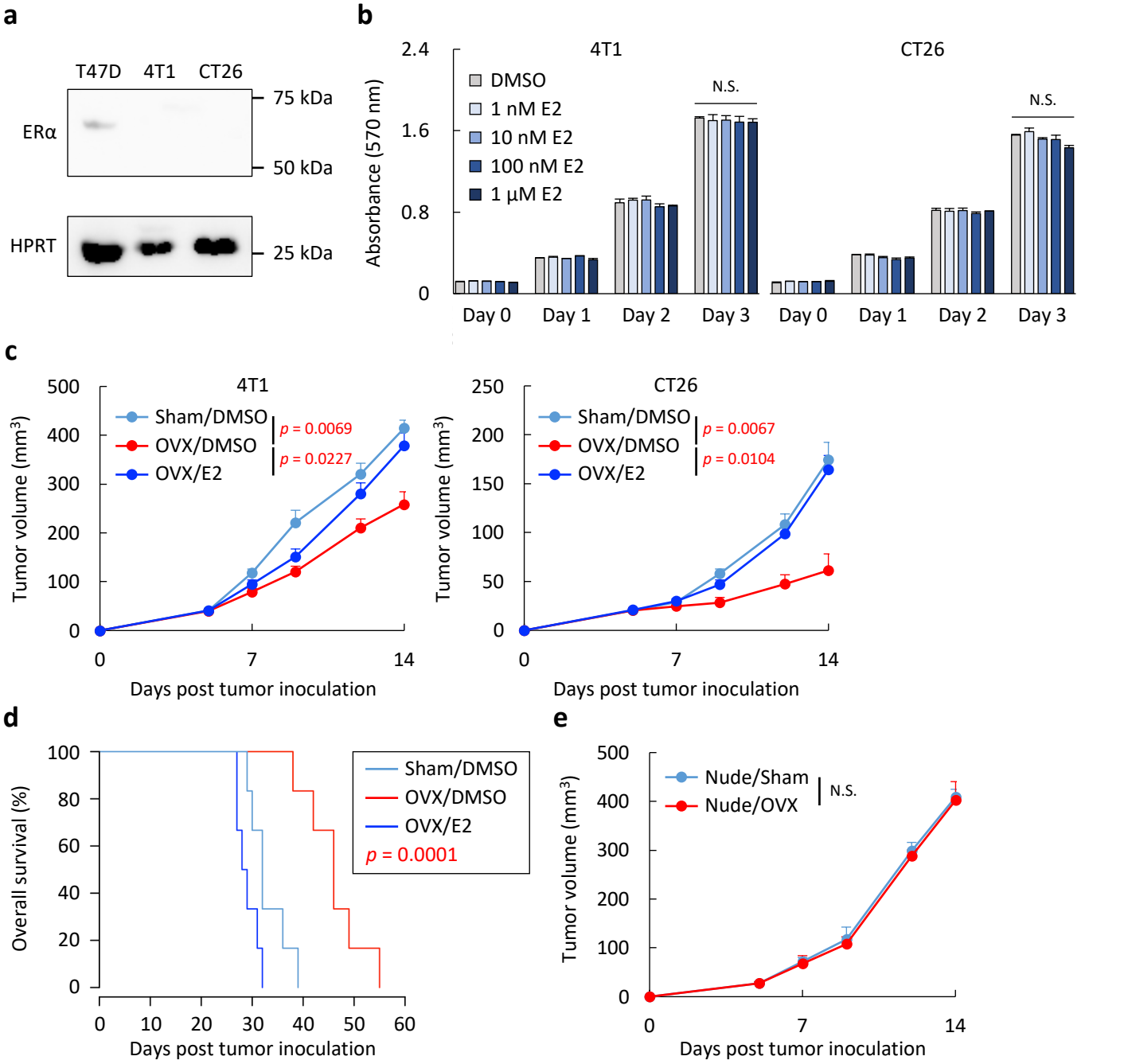
(a) Subcutaneous tumor growth in BALB/c mice inoculated with 4T1 or CT26 cells ($1x10^5$ and $2x10^5$ cells, respectively, n=3-4) and treated with dimethyl sulfoxide (DMSO) or fulvestrant (FUL) and anti-CTLA-4 antibody (αCTLA-4) or isotype control (IgG). Bar graphs represent each group's tumor volume 14 days post tumor development. (b) Subcutaneous tumor growth

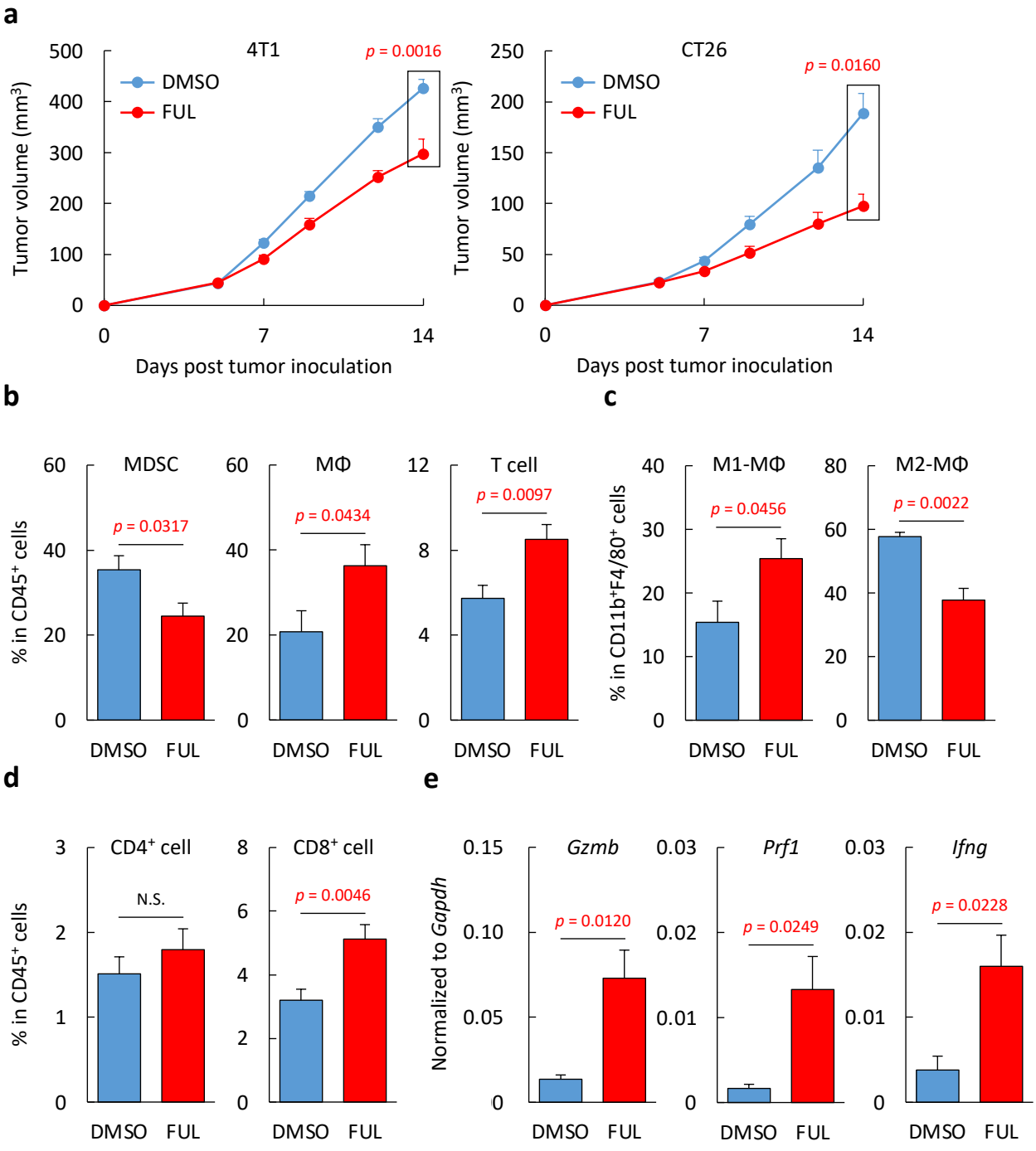
in BALB/c mice inoculated with 4T1 or CT26 cells ($1x10^5$ and $2x10^5$ cells, respectively, n=3-4) and treated with DMSO or FUL and anti-PD-1 antibody (αPD-1) or IgG. Bar graphs represent each group's tumor volume 14 days post tumor development. (c) Subcutaneous tumor growth in BALB/c mice inoculated with 4T1 cells ($1x10^5$ cells, n=4) and treated with DMSO or FUL and αCTLA-4 plus αPD-1 or IgG. Bar graphs represent each group's tumor volume 14 days post tumor development. (d) Bar graphs represent the frequency of $CD3^+CD69^+$ cells and $CD8^+CD69^+$ cells within $CD45^+$ cells infiltrated in the 4T1 tumors (n=4). Values were analyzed by a Tukey-Kramer test and are shown as mean±SEM.

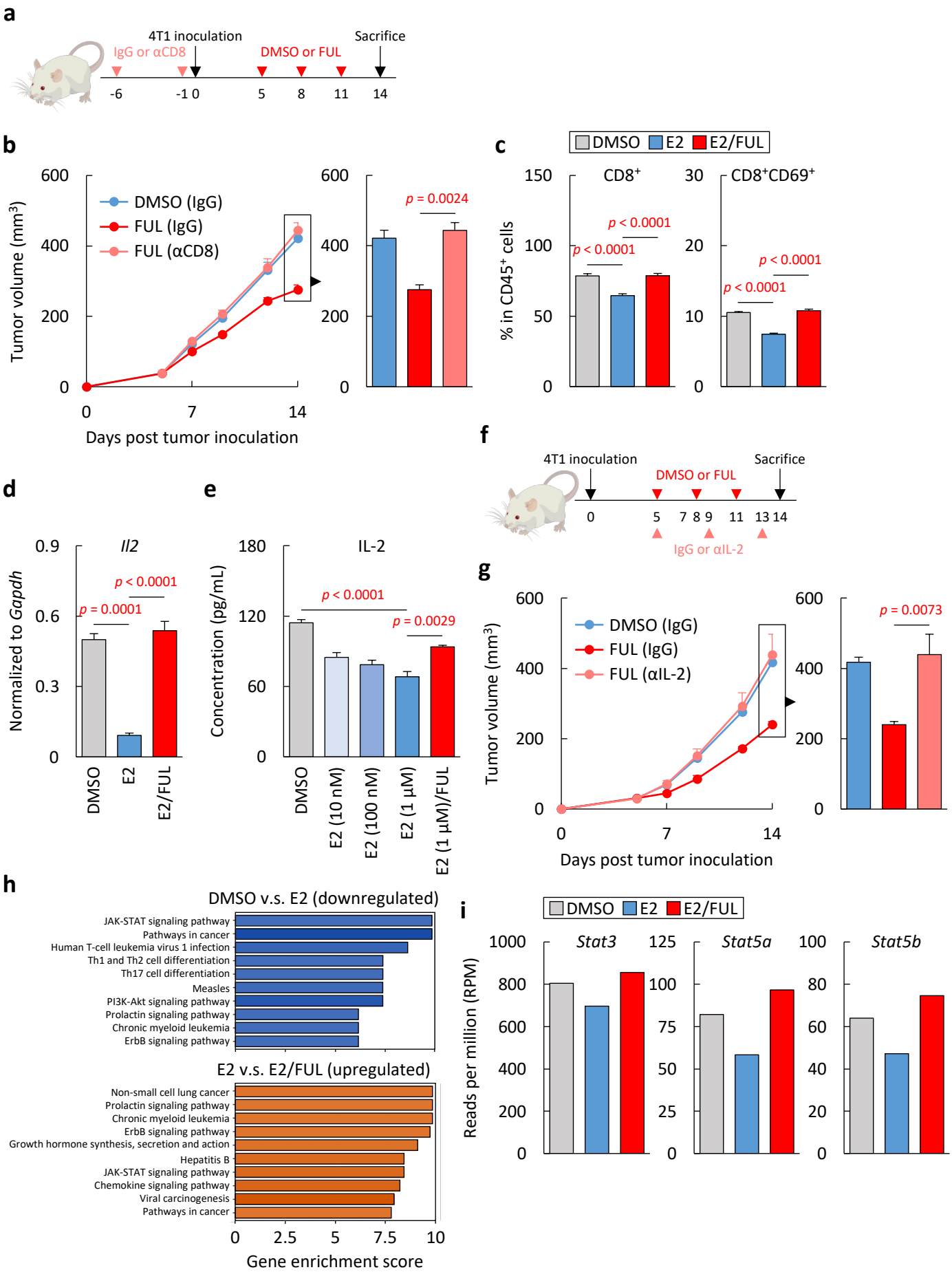
Figure 6: Effects of fulvestrant combined with immune checkpoint inhibitors and chemotherapy on ERα-negative tumor growth.

(a) Subcutaneous tumor growth in BALB/c mice inoculated with 4T1 cells ($1x10^5$ cells, n=4) and treated with dimethyl sulfoxide (DMSO) or fulvestrant (FUL) and anti-CTLA-4 antibody (αCTLA-4) and anti-PD-1 antibody (αPD-1) or isotype control (IgG) and paclitaxel (PTX) or saline. Bar graphs represent each group's tumor volume 14 days post tumor development. (b) Bar graphs represent the frequency of $CD3^+$ T cells, $CD3^+CD69^+$ T cells, $CD8^+$ T cells ($CD3^+CD8^+$ cells), and $CD8^+CD69^+$ T cells ($CD3^+CD8^+CD69^+$ cells) within $CD45^+$ cells infiltrated in the 4T1 tumors (n=4). Values were analyzed by a Tukey-Kramer test and are shown as mean±SEM.


a
HSD17B1 expression level
Rho = -0.160
p = 2.72e-02
PRF1 expression level
Rho = -0.175
p = 1.57e-02
GZMB expression level
Rho = -0.201
p = 5.34e-03
IFNG expression level
Rho = -0.188
p = 9.23e-03
CD3E expression level
Rho = -0.187
p = 9.60e-03
CD69 expression level
Rho = -0.224
p = 1.82e-03
CD8A expression level
b
Rho = -0.299
p = 6.05e-05
CD8+ T cell infiltration level
c
CD8+ T cell infiltration level
p = 0.0048
Low
High
HSD17B1
d
Survival (%)
Low HSD17B1
High HSD17B1
p = 0.0171
Time to follow-up (months)


a
T47D
4T1
CT26
ERα
75 kDa
50 kDa
HPRT
25 kDa
b
4T1
CT26
DMSO
1 nM E2
10 nM E2
100 nM E2
1 μM E2
Absorbance (570 nm)
N.S.
Day 0
Day 1
Day 2
Day 3
c
4T1
CT26
Sham/DMSO
OVX/DMSO
OVX/E2
p = 0.0069
p = 0.0227
p = 0.0067
p = 0.0104
Tumor volume (mm3)
Days post tumor inoculation
d
Overall survival (%)
Sham/DMSO
OVX/DMSO
OVX/E2
p = 0.0001
Days post tumor inoculation
e
Nude/Sham
Nude/OVX
N.S.
Tumor volume (mm3)
Days post tumor inoculation


a
4T1
p = 0.0016
DMSO
FUL
Tumor volume (mm3)
Days post tumor inoculation
CT26
p = 0.0160
b
MDSC
p = 0.0317
MΦ
p = 0.0434
T cell
p = 0.0097
% in CD45+ cells
c
M1-MΦ
p = 0.0456
M2-MΦ
p = 0.0022
% in CD11b+F4/80+ cells
d
CD4+ cell
N.S.
CD8+ cell
p = 0.0046
e
Gzmb
p = 0.0120
Prf1
p = 0.0249
Ifng
p = 0.0228
Normalized to Gapdh


a
4T1 inoculation
IgG or αCD8
DMSO or FUL
Sacrifice
-6
-1 0
5
8
11
14
b
Tumor volume (mm³)
DMSO (IgG)
FUL (IgG)
FUL (αCD8)
Days post tumor inoculation
p = 0.0024
c
DMSO
E2
E2/FUL
% in CD45⁺ cells
CD8⁺
CD8⁺CD69⁺
p < 0.0001
p < 0.0001
p < 0.0001
p < 0.0001
d
Il2
Normalized to Gapdh
p < 0.0001
p = 0.0001
DMSO
E2
E2/FUL
e
IL-2
Concentration (pg/mL)
p < 0.0001
p = 0.0029
DMSO
E2 (10 nM)
E2 (100 nM)
E2 (1 μM)
E2 (1 μM)/FUL
f
4T1 inoculation
DMSO or FUL
Sacrifice
0
5
7 8 9
11
13 14
IgG or αIL-2
g
Tumor volume (mm³)
DMSO (IgG)
FUL (IgG)
FUL (αIL-2)
Days post tumor inoculation
p = 0.0073
h
DMSO v.s. E2 (downregulated)
JAK-STAT signaling pathway
Pathways in cancer
Human T-cell leukemia virus 1 infection
Th1 and Th2 cell differentiation
Th17 cell differentiation
Measles
PI3K-Akt signaling pathway
Prolactin signaling pathway
Chronic myeloid leukemia
ErbB signaling pathway
E2 v.s. E2/FUL (upregulated)
Non-small cell lung cancer
Prolactin signaling pathway
Chronic myeloid leukemia
ErbB signaling pathway
Growth hormone synthesis, secretion and action
Hepatitis B
JAK-STAT signaling pathway
Chemokine signaling pathway
Viral carcinogenesis
Pathways in cancer
Gene enrichment score
i
DMSO
E2
E2/FUL
Reads per million (RPM)
Stat3
Stat5a
Stat5b

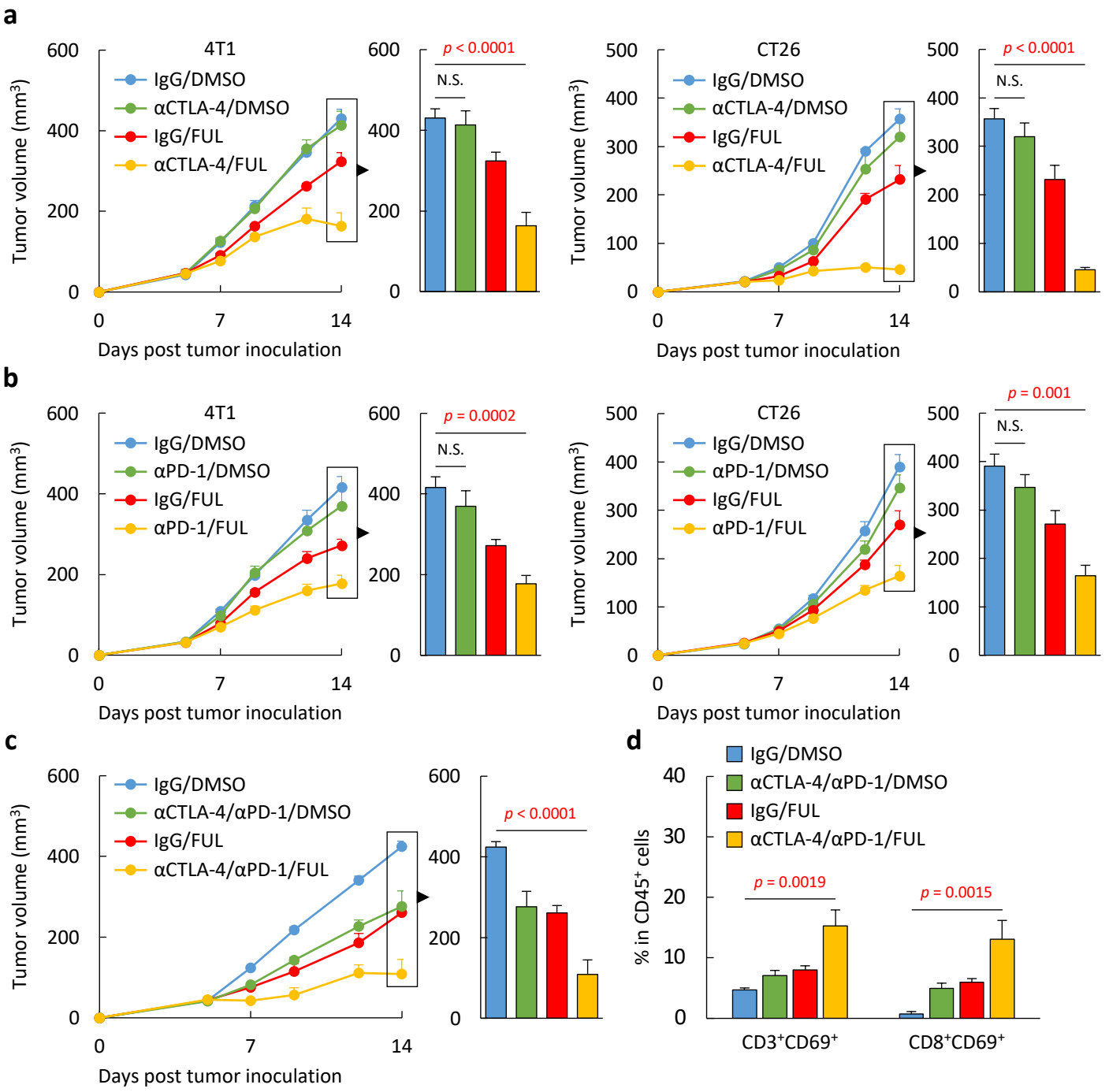
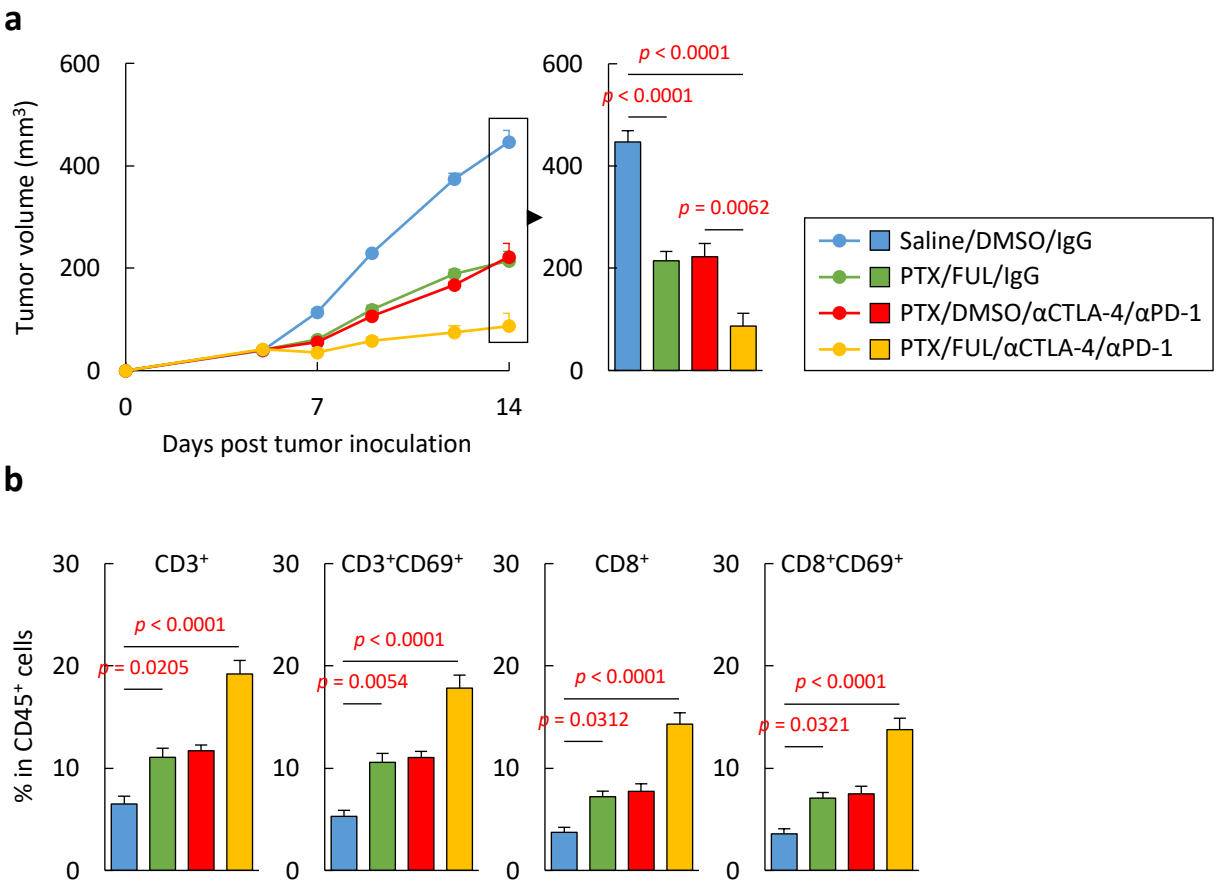

a
4T1
IgG/DMSO
αCTLA-4/DMSO
IgG/FUL
αCTLA-4/FUL
Tumor volume (mm³)
Days post tumor inoculation
p < 0.0001
N.S.
CT26
b
αPD-1/DMSO
αPD-1/FUL
p = 0.0002
p = 0.001
c
αCTLA-4/αPD-1/DMSO
αCTLA-4/αPD-1/FUL
d
% in CD45⁺ cells
p = 0.0019
p = 0.0015
CD3⁺CD69⁺
CD8⁺CD69⁺

Fig. 6


a
Tumor volume (mm3)
600
400
200
0
0
7
14
Days post tumor inoculation
p < 0.0001
p < 0.0001
p = 0.0062
Saline/DMSO/IgG
PTX/FUL/IgG
PTX/DMSO/αCTLA-4/αPD-1
PTX/FUL/αCTLA-4/αPD-1
b
% in CD45+ cells
CD3+
CD3+CD69+
CD8+
CD8+CD69+
30
20
10
0
p < 0.0001
p = 0.0205
p < 0.0001
p = 0.0054
p < 0.0001
p = 0.0312
p < 0.0001
p = 0.0321